

# Crystal Structure of a Bacterial Endospore Coat Component

A LACCASE WITH ENHANCED THERMOSTABILITY PROPERTIES\*

Received for publication, February 5, 2003, and in revised form, March 3, 2003  
Published, JBC Papers in Press, March 13, 2003, DOI 10.1074/jbc.M301251200

Francisco J. Enguita<sup>‡§</sup>, Lígia O. Martins<sup>‡¶</sup>, Adriano O. Henriques<sup>‡</sup>,  
and Maria Arménia Carrondo<sup>‡||</sup>

From the <sup>‡</sup>Instituto de Tecnologia Química e Biológica, Universidade Nova de Lisboa, 2781-901 Oeiras and  
<sup>¶</sup>Universidade Lusófona de Humanidades e Tecnologias, Departamento de Engenharias e Tecnologias,  
Avenida do Campo Grande, 376, 1749-024 Lisbon, Portugal

Endospores produced by the Gram-positive soil bacterium *Bacillus subtilis* are shielded by a proteinaceous coat formed by over 30 structural components, which self-assemble into a lamellar inner coat and a thicker striated electrodense outer coat. The 65-kDa CotA protein is an abundant component of the outer coat layer. CotA is a highly thermostable laccase, assembly of which into the coat is required for spore resistance against hydrogen peroxide and UV light. Here, we report the structure of CotA at 1.7-Å resolution, as determined by x-ray crystallography. This is the first structure of an endospore coat component, and also the first structure of a bacterial laccase. The overall fold of CotA comprises three cupredoxin-like domains and includes one mononuclear and one trinuclear copper center. This arrangement is similar to that of other multicopper oxidases and most similar to that of the copper tolerance protein CueO of *Escherichia coli*. However, the three cupredoxin domains in CotA are further linked by external interdomain loops, which increase the packing level of the structure. We propose that these interdomain loops contribute to the remarkable thermostability of the enzyme, but our results suggest that additional factors are likely to play a role. Comparisons with the structure of other monomeric multicopper oxidases containing four copper atoms suggest that CotA may accept the largest substrates of any known laccase. Moreover, and unlike other laccases, CotA appears to have a flexible lidlike region close to the substrate-binding site that may mediate substrate accessibility. The implications of these findings for the properties of CotA, its assembly and the properties of the bacterial spore coat structure are discussed.

such as hydrogen peroxide and lysozyme, at levels that would promptly destroy the corresponding vegetative cells (1, 2). One of the parameters that decisively contributes to their remarkable resistance properties is the organization and composition of the protective layers that encase the mature spore (1, 2). The spore core that contains a copy of the genome is surrounded by a layer of modified peptidoglycan called the cortex, which is essential for heat resistance. The cortex is protected from the action of lytic enzymes by a proteinaceous coat, which also confers resistance to noxious chemicals and to UV light, and allows the prompt response of spores to germinants (1–3). In the model organism *Bacillus subtilis*, the spore coat is composed of over 30 different protein components, which are arranged in a lamellar inner coat and a striated electrodense outer coat (1, 2). Synthesis of the coat polypeptides is temporally and spatially regulated by the successive appearance of four mother cell-specific transcriptional regulators, in the order  $\sigma^E$ , SpoIIID,  $\sigma^K$ , and GerE (1, 2, 4, 5). However, the ordered assembly of the coat components appears to rely mostly upon post-transcriptional and post-translational mechanisms such as alternative translation initiation, protein secretion, cross-linking, or proteolysis, which enforce the correct interactions among the various coat components (1, 2, 6). Assembly of the spore coat also relies on the action of a class of unique morphogenetic proteins, which act by guiding the assembly of several coat components (1, 2, 7). CotE, for example, is a morphogenetic protein required for the assembly of the spore outer coat layer (8) and may act in part by directly interacting with and recruiting several of the outer coat proteins (9).

Despite its importance as a model system for studying the assembly of a multiprotein structure, as a platform for the display of heterologous enzymes or antigens, in pathogenesis and host immune response, and possibly in mediating the germination of spores in the gastrointestinal tract (2, 10, 11), our knowledge of the molecular mechanisms underlying the assembly of the bacterial spore coat is still scarce. The function of individual coat components is largely unknown, and in only a few cases have the interactions relevant for their assembly been unraveled. For example, a putative manganese catalase, CotJC, interacts with a smaller protein (CotJA) to form a complex that is targeted to the inner coat layers (12, 13). Another case involves the SafA and SpoVID morphogenetic proteins. SpoVID and SafA interact directly, and the targeting of SafA to the surface of the developing spore requires SpoVID (6, 14). However, the nature of these interactions and the structural basis for the assembly of the resulting complexes are unknown. Evidently, more detailed studies are needed to understand the mechanisms by which specific proteins or protein complexes are targeted to the nascent coat. In an attempt to begin addressing these questions, we have initiated the struc-

---

Bacterial endospores are differentiated cell types that can withstand exposure to a wide range of physical agents including heat, desiccation, radiation, and UV light, and to chemicals

---

\* The costs of publication of this article were defrayed in part by the payment of page charges. This article must therefore be hereby marked "advertisement" in accordance with 18 U.S.C. Section 1734 solely to indicate this fact.

The atomic coordinates and structure factors (code 1GSK) have been deposited in the Protein Data Bank, Research Collaboratory for Structural Bioinformatics, Rutgers University, New Brunswick, NJ (<http://www.rcsb.org/>).

§ Supported by an EMBO long term fellowship followed by a PRAXIS XXI postdoctoral fellowship (Fundação para a Ciência e a tecnologia, Ministério de Ciência e Tecnologia, Portugal).

|| To whom correspondence should be addressed: Protein Crystallography Laboratory, Instituto de Tecnologia Química e Biológica, 2781-901 Oeiras, Portugal. Tel.: 351-21-4469657; Fax: 351-21-4433644; E-mail: carrondo@itqb.unl.pt.

tural characterization of selected spore coat components. The CotA<sup>1</sup> protein is a 65-kDa abundant component of the outer coat layer (15), recently shown to possess copper-dependent laccase activity and to be highly thermostable (3, 16).

Laccases are polyphenol oxidases, able to oxidize a wide range of substrates, including xenobiotic compounds such as methoxyphenols, anilines, and benzenethiols (17), and belong to the multicopper oxidase family, characterized by the presence of one mononuclear and one trinuclear copper site. The multicopper oxidase family also groups ascorbate oxidase (18), ceruloplasmin (19), various manganese oxidases (20), and other enzymes involved in copper and iron metabolism, including CueO from *Escherichia coli* (21) and Fet3p from *Saccharomyces cerevisiae* (22). In plants laccases are involved in cell wall formation, whereas in fungi they are involved in lignin degradation, detoxification and pathogenesis (23). Besides *B. subtilis*, laccase activity was also found in two other bacterial species, the soil bacterium *Azospirillum lipoferum* (24), and the marine bacteria *Marinomonas mediterranea* (25). Moreover, putative laccase-like multicopper oxidases have been detected in the genomes of other bacterial species, suggesting that laccases are widespread in bacteria (26). However, of the three laccases that have been structurally characterized, those from *Coprinus cinereus* (27), from *Trametes versicolor* (28), and from *Melanocarpus albomyces* (29), none is of bacterial origin. Laccases have been the subject of increasing attention because of their established or potential novel uses in biotechnology (see Ref. 28 and references therein), but they are also an important system for studying the mechanism of oxidation reactions involving transfer of four single electrons from the substrate to the final acceptor (30).

The exact function of CotA within the spore coat is still not fully understood, but the assembly of CotA is essential for the full complement of spore resistance properties. Expression of the *cotA* gene has been classically implicated in the biosynthesis of a brownish pigment that characterizes sporulating colonies of *B. subtilis*, and which has properties of a melanin and appears to confer protection against UV light (3, 15, 31). Expression of *cotA* is also required for the resistance of spores to hydrogen peroxide (32). Because of its importance for the resistance properties of the spore structure, because of the importance of laccases, and unique thermostability of CotA among this class of enzymes (16), we began the structural characterization of relevant components of the spore coat, by focusing our attention on CotA. In this paper we describe the three-dimensional structure of the *B. subtilis* CotA laccase, as determined by x-ray crystallography. This is the first report on the structure of a bacterial endospore component, and also the first structure of a bacterial laccase.

#### EXPERIMENTAL PROCEDURES

**Protein Purification and Crystallization**—Purification of recombinant CotA was performed essentially as described previously (16), using an *E. coli* overproducing host. Protein crystals were grown at 293 K, by the vapor diffusion method, using 10–15 mg/ml purified CotA protein, and a reservoir solution containing 100 mM sodium citrate buffer (pH = 5.5), 15% glycerol, 12–15% isopropanol, and 12–15% polyethylene glycol 4000 (33).

**Data Collection and Structure Solution**—CotA crystals reached maximum dimensions of  $0.2 \times 0.3 \times 0.5$  mm, showing a hexagonal prismatic shape, and the characteristic blue color caused by the presence of

type I copper centers within the protein (33). They belong to P3<sub>2</sub>1 spacegroup with cell dimensions of  $a = b = 101.8$  Å,  $c = 136.1$  Å, and one protein molecule per asymmetric unit, corresponding to a solvent content of 55%.

Diffraction data were collected from two crystals: one considered as a “native” for high resolution data collection, and the other one for structure solution by the multiwavelength anomalous dispersion method (MAD). Data collection for the “native” data set was performed at the ID-14-EH2 beamline (ESRF, Grenoble, France), and the MAD experiment was undertaken at the BW7A beamline (EMBL, Hamburg, Germany). The structure was solved by the MAD method at the copper K edge, using the anomalous signal of the copper atoms within the structure (33). Automated interpretation of anomalous Patterson maps by SOLVE (34) allowed the localization of two copper atoms: type I copper, and one of the copper atoms belonging to the binuclear type III center. The positions of the two remaining copper atoms were determined using the corresponding anomalous difference maps, calculated with the initial phases. Electron density maps were improved by density modification with RESOLVE (35).

**Model Building and Refinement**—The original phases obtained with data to 2.65-Å resolution, derived from anomalous Patterson maps interpretation and density modification by SOLVE-RESOLVE (34, 35), were extended to 1.7-Å resolution using the maximum resolution data set available with DM (36). Using this extended phase information, initial model building was performed automatically using ARP/WARP version 5.1 (37). After 50 cycles of refinement and 10 cycles of building, 93% (479 of 513 possible) of the protein residues were found, and placed in seven chains, with a global connectivity index of 0.97. At the end of the automatic building procedure, the refinement converged to an  $R$  factor of 20.2% and an  $R_{\text{free}}$  factor of 24.5%. The amino acid side chains built with the *side\_dock* script included in the ARP/WARP suite, had a confidence factor of 0.95. After this process, manual intervention was required to complete the model. Missing sections were built from  $2F_o - F_c$  maps using Xtalview (38). The Xtalview suite was also employed to complete the solvent boundary of the protein model, including four glycerol molecules belonging to the crystallization buffer and located mainly at the surface of the protein.

Protein chain and solvent molecules were input to REFMAC5 for refinement (39). Positional and isotropic thermal parameters were refined individually for each atom to a resolution limit of 1.7 Å. During the initial refinement steps, isotropic thermal parameters of atoms belonging to the type II and III copper centers refined to values close to 80 Å<sup>2</sup>, probably because of the low copper content of the protein crystals. For this reason, occupancies for atoms belonging to the trinuclear T2/T3 copper center were maintained at 0.5. After several cycles of refinement and model checking the refinement converged to a  $R$  factor of 17.7% and a  $R_{\text{free}}$  factor of 19.8%. No electron density was visible in the region comprising residues 90–96, which lie in an apparently disordered loop, the initial methionine, and also the C-terminal last three residues. The final model contained 502 of the 513 residues in the primary sequence of CotA. The stereochemistry of the final model was analyzed with PROCHECK (40) and WHATIF (41). The overall mean  $B$  factor of the structure after refinement was 25.82 Å<sup>2</sup>, and root mean square deviations from ideal values were 0.019 Å for bond lengths, and 1.837° for bond angles (see Table I for additional details of the refinement).

**Other Methods**—Surface calculations were performed by MSMS (42), and putative substrate binding pockets were determined using the CASTP server (43). All the graphical representations of CotA or other multicopper oxidases were made using PyMol (44). Domain analysis based on the quantification of local atomic interactions was performed by using DOMID server (45). Residue packing in CotA was estimated by calculating the normalized occluded surface packing value (OSP) using by the program OS (46). Fig. 2 was prepared by ESPrnt (47) using MULTALIN as alignment program (48).

#### RESULTS

**Overall Structure of CotA**—CotA is a monomeric protein (16) and has the overall dimensions  $70 \times 50 \times 20$  Å (Fig. 1, panel A). The overall CotA fold comprises three cupredoxin-like domains, as shown in Figs. 1 (panel A) and 2. This fold was first observed in the small blue copper proteins plastocyanin and azurin (49), and subsequently detected in other more complex multicopper enzymes (21, 27). The cupredoxin fold is mainly formed by an eight-stranded Greek key  $\beta$ -barrel, comprising two  $\beta$ -sheets composed by four strands, arranged in a sandwich conformation (50). The first (N-terminal, domain 1; represented in blue

<sup>1</sup> The abbreviations used are: CotA, *B. subtilis* CotA (PDB code 1GSK); CueO, *E. coli* CueO (PDB code 1KV7); CeLa, *C. cinereus* laccase (PDB code 1A65); TvLa, *T. versicolor* laccase (PDB code 1KYA); MaLa, *M. albomyces* laccase (PDB code 1GW0); Asox, zucchini ascorbate oxidase (PDB code 1AOZ); PDB, Protein Data Bank; MAD, multiwavelength anomalous dispersion; OSP, normalized occluded surface packing value.

TABLE I  
Refinement statistics obtained using REFMAC\_5 (39) for the final CotA model

Values in parentheses correspond to the last resolution shell.

Spacegroup	P3 <sub>1</sub> 21
Cell dimensions	$a = 102.051, b = 102.051, c = 136.393, \alpha = 90.00, \beta = 90.00, \gamma = 120.00$
No. of reflexions	86,412
No. of protein atoms	4044
No. of solvent atoms	480
No. of heterogen atoms	30
Resolution range for refinement (Å)	87.71–1.70 (1.78–1.70)
Completeness for range	99.8 (89.5)
$R_{\text{cryst}}$	17.76 (19.85)
$R_{\text{free}}$	19.85 (22.10)
Overall B value of the model (Å <sup>2</sup> )	25.82
Correlation coefficient $F_o - F_c$	0.965
Correlation coefficient $F_o - F_c$ Free	0.959
Root mean square bond lengths deviation (Å)	0.019
Root mean square bond angles deviation (degrees)	1.837

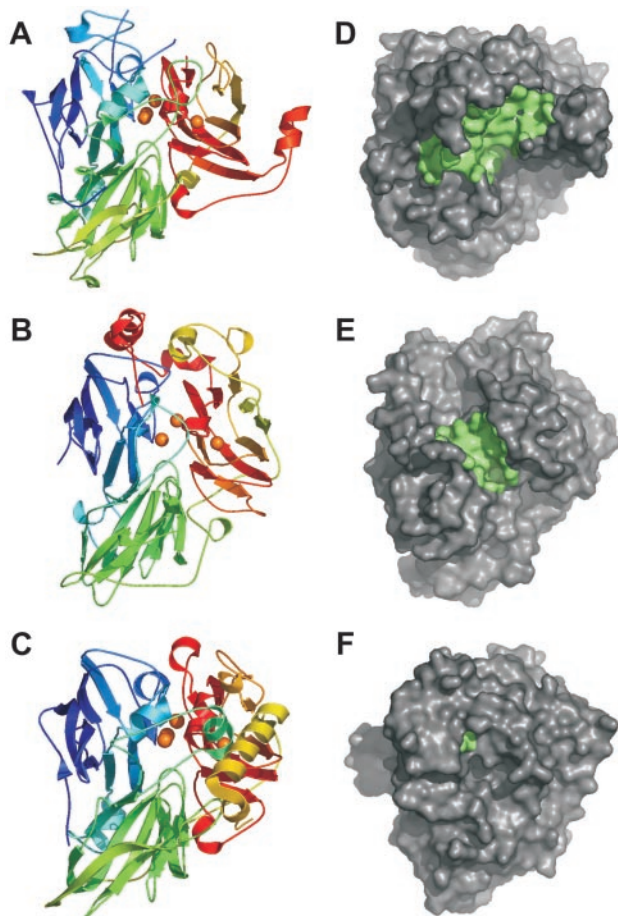


FIG. 1. Overall structure and putative substrate binding pockets of selected multicopper oxidases. Surface calculations were performed by MSMS (42) and putative substrate binding pockets were determined using the CASTP server (43) as described under “Experimental Procedures.” All the molecular representations were generated using PyMol (44). Left column, a rainbow-colored (from N terminus in blue to C terminus in red) ribbon representation of CotA (A), CcLa (B), and CueO (C) is shown, including the localization of the copper atoms within the structure (plotted as orange balls). In panel A, the lidlike structure over the putative substrate-binding site in CotA is visible to the right. Right column, molecular surface representation of CotA (D), CcLa (E), and CueO (F) with the putative substrate binding pocket colored in green. The view in panels D and E represents a 45° clockwise rotation relative to the left column view, and was intended to facilitate the observation of the putative substrate binding site cavities.

in Fig. 1A) cupredoxin-like domain of CotA (residues 2–176; Fig. 2) has a somewhat distorted conformation in comparison with the equivalent domain in other multicopper oxidases. It

comprises eight strands organized in a  $\beta$ -barrel form, starting with a coiled section (residues 2–25; Fig. 2) that connects domains 1 and 2, and is stabilized by hydrogen bonds, contributing to the packing between these domains. This coiled section is absent in plant and fungal multicopper oxidases such the laccase from *C. cinereus* (CcLa; Fig. 1B) (27) and ascorbate oxidase (Asox) (18). However, a similar coiled section is present in the *E. coli* CueO protein (Figs. 1C and 2) (21).

The overall fold of the second cupredoxin-like domain of CotA (domain 2, represented in green in Fig. 1A) comprises a  $\beta$ -barrel composed by 12 strands (residues 183–340; Fig. 2), very similar to the fold of domain 2 in Asox (18). Domain 2 of CotA acts as a bridge between domains 1 and 3 (Fig. 1A), but a short  $\alpha$ -helical fragment, encompassing residues 177–182, makes the connection between domains 1 and 2, whereas a large loop segment including residues 341–368 links domains 2 and 3 (Figs. 1A and 2). In both the structures of CotA and CueO, this region represents an external connection between domains 2 and 3, whereas in plant and fungal multicopper oxidases the corresponding link is made through an internal connection (compare the structures of CotA and CueO in Fig. 1 (A and C, respectively) with that of CcLa in Fig. 1B). Therefore, this feature may be a characteristic of the prokaryotic variants of these enzymes. Together with the coiled section that links domains 1 and 2 of CotA (which also has an equivalent in CueO; see above), this external loop motif contributes decisively to the closer resemblance between the overall folds of the prokaryotic proteins CotA and CueO, relative to other structurally characterized multicopper oxidases (see also below).

Finally, domain 3 of CotA (in red in Fig. 1A; residues 369–501 in Fig. 2) not only contains the mononuclear copper center, but also contributes to the formation of the binding site of the trinuclear copper center, which is located in the interface between domains 1 and 3 (Fig. 1A). Moreover, domain 3 includes the putative substrate binding site, located at the surface of the protein, close to the type I mononuclear copper center (see Fig. 1, A and D). A protruding section formed by a loop and a short  $\alpha$ -helix (Fig. 1), comprising amino acids from 434 to 454 (Fig. 2), forms a lid-like structure over the substrate binding site. No similar element has been found in the previously analyzed multicopper oxidases with known three-dimensional structure. Therefore, this structural element represents a distinctive feature of CotA.

**Comparison with Other Multicopper Oxidases**—The primary sequence of CotA was aligned with that of all the monomeric multicopper oxidases of known three-dimensional structures: CueO (PDB code 1KV7), the laccases CcLa (PDB code 1A65), TvLa (PDB code 1KYA), MaLa (PDB code 1GW0), and Asox (PDB code 1AOZ) (Fig. 2). The copper binding motives are

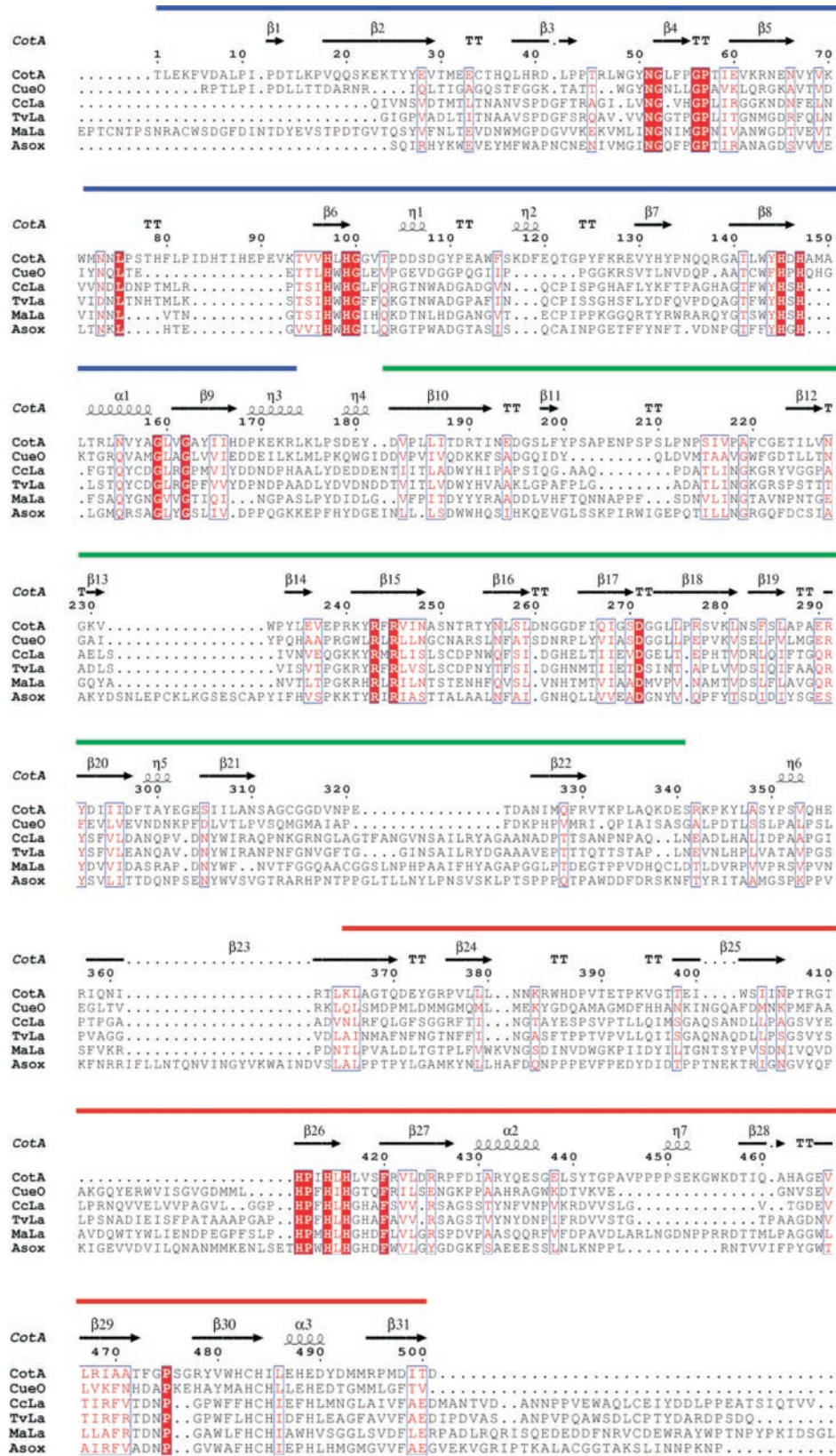


FIG. 2. Sequence alignment by MULTALIN (48) of monodomain multicopper oxidases containing four copper atoms and with known three-dimensional structure. Highly conserved regions are boxed. Within those, invariant residues are represented against a red background, whereas conserved residues are shaded. The secondary structure of CotA as derived from the three-dimensional data is represented in the upper part of the alignment. The CotA domains are also represented as different colored solid bars over the secondary structure.

conserved in all sequences. Further similarities are more significant in the N- and C-terminal regions, corresponding to domains 1 and 3 in the CotA structure (see above). CotA has an

insertion between residues 80 and 90, which unfortunately could not be structurally characterized because of the lack of electron density in this region. A C-terminal extension of ~30

TABLE II

Statistics of three-dimensional alignment by least squares superposition of C- $\alpha$  atoms, of selected monomeric multicopper oxidases with four copper atoms, as performed by MODELLER version 6 (51)

Diagonal bold row, total number of residues on each PDB file; rows above diagonal, root mean square ( $\text{\AA}$ ) of the alignment; rows below diagonal, number of residues in equivalent spatial positions.

	CotA	CueO	CcLa	TvLa	MaLa	Asox
CotA	<b>502</b>	1.639	1.879	1.949	2.084	2.109
CueO	404	<b>463</b>	2.042	1.979	2.097	2.045
CcLa	371	365	<b>504</b>	0.949	1.614	1.587
TvLa	370	363	489	<b>499</b>	1.565	1.586
MaLa	364	355	447	449	<b>559</b>	1.770
Asox	369	362	428	431	458	<b>463</b>

residues present in the fungal and plant variants of these proteins is absent from the two bacterial multicopper oxidases, CotA and CueO. To determine the structural similarities among the analyzed enzymes, a C $\alpha$  alignment was generated with version 6 of MODELLER (51). The results of this comparison are presented in Table II. In agreement with the conservation of particular structural elements between CotA and CueO (see above), these results indicate that from a structural point of view, CotA is more closely related to the *E. coli* CueO protein (21), with a root mean square of 1.639  $\text{\AA}$  for the superposition of C $\alpha$  carbons, than to the other analyzed monomeric multicopper oxidases.

**Copper Centers**—The copper sites in multicopper oxidases are classified into three main classes on the basis of their spectroscopic properties. Type I copper has a distorted bipyramidal trigonal coordination, with two histidines and a cysteine as conserved ligands and one position usually vacant. The axial ligand is usually a methionine or an aliphatic amino acid, and is a major determinant in the redox potential of the site (52). Type I copper is also termed the “blue” copper site, as it confers the typical blue color to proteins of this family. This results from the intense ( $\epsilon \approx 5,000 \text{ M}^{-1}\text{cm}^{-1}$ ) electronic absorption around 600 nm wavelength that originates from the highly covalent Cu  $d_x^2 - y^2$  Cys S  $\rho_\pi$  bond. Type I copper is paramagnetic, with an EPR spectrum characterized by an unusually low value of the copper hyperfine coupling constant in the parallel region. Type II copper does not appreciably contribute to the absorption spectrum of the protein, and its EPR profile shows magnetic parameters in line with those of the vast majority of copper complexes. In multicopper oxidases, type II copper is strategically positioned close to the third type (type III center) of copper, a binuclear center, spectroscopically characterized by an electronic absorption at 330 nm and by the absence of an EPR signal as the result of the antiferromagnetic coupling between two copper ions. Type II and type III copper can be regarded as a whole, and for this reason they are often referred to as a “trinuclear cluster.” From the functional point of view, the various copper centers within multicopper oxidases act to drive electrons from a reducing substrate to molecular oxygen, in a controlled manner, without releasing potential toxic intermediates such as  $\text{O}_2^-$  or  $\text{H}_2\text{O}_2$  (53). This task is accomplished through monoelectronic oxidations of the substrate catalyzed by the type I copper center, that shuttles electrons from the substrate to the trinuclear cluster, where reduction of molecular oxygen and release of water takes place (30).

The geometry and electron density defining the copper centers in CotA can be seen in Fig. 3. Table III lists the bonding distances in the CotA structure and the other proteins herein used for structural comparisons: CueO, CcLa, TvLa, and Asox (18, 21, 27–29, 54). The mononuclear type I copper site in CotA has the typical geometry found for this site in other multicopper oxidases, with two histidines, one cysteine, and a methionine displaying a distorted bipyramidal geometry and an additional vacant axial position for the binding of the reducing

substrate (Fig. 3A). The fungal laccases have an aliphatic residue as the distant axial ligand in contrast with the situation observed in CotA, Asox, and CueO, where this residue is a methionine. The trinuclear copper center is normally coordinated by eight histidines, using a pattern of four His-X-His motifs. In CotA, the type III copper atoms (Cu2 and Cu3) are coordinated by six of these histidines, and the remaining two histidines are involved in the coordination of type II copper (Cu4) (Fig. 3A). In terms of geometry, the coordination of type III copper atoms by three histidines is comparable to that observed in other multicopper oxidases. It is interesting to note that one of these ligands (His<sup>107</sup> in CotA) is bound in all the known structures to Cu2 through its N $\delta$  atom. The CcLa laccase has, however, a unique situation regarding the type III site, as its Cu3 atom shows a fourth coordinating histidine and an asymmetric hydroxyl bridge between Cu2 and Cu3 (27). The strong antiferromagnetic coupling between the two type III copper atoms is maintained by an hydroxyl ligand, which acts as a bridge between the copper atoms (52).

The hydroxyl bridge between the type III copper atoms is (Fig. 3A) in an almost linear arrangement as observed in the structures of TvLa and CueO (21, 28, 54). Quite interestingly, the type II Cu atom (Cu4) in the CotA structure (Fig. 3A) is at a significantly longer distance to the two type III coppers than in all other structures listed in Table III. Even in the case of the MaLa laccase structure, which displays a dioxygen molecule in the middle of the trinuclear copper center, the corresponding distances are comparable to those observed in all other structures (18, 21, 27–29, 54). These long distances between Cu4 and its neighboring Cu atoms in CotA, coupled with a typical oxidized Cu2 . . . Cu3 distance, may be an indication of a reduced state on this copper site. This inference is in agreement with the EPR spectra of CotA, which shows no signal caused by the copper type II site.<sup>2</sup> Longer Cu . . . Cu distances were observed in the case of the reduced structure of Asox (55) with Cu . . . Cu distances in the trinuclear center of 4.1, 4.5, and 5.1  $\text{\AA}$ , this latter corresponding to the Cu2 . . . Cu3 distance. Also, in the structure of CcLa, where only type I and III copper atoms are present, the distance between the Cu atoms in the type III center is 4.9  $\text{\AA}$ , an observation that prompted the authors to assume a reduced state for this pair (55).

**Solvent Channels**—Laccases catalyze the oxidation of different substrates via monoelectronic oxidations at type I copper center. These electrons are transferred to a dioxygen molecule to generate water by the trinuclear copper center (30). In all available laccase structures, the trinuclear copper center is located in a central cavity of the enzyme formed at the interface between domains 1 and 2 (27, 28). The access of molecular oxygen to the trinuclear copper center in CotA is granted by the presence of at least two clear solvent channels formed mainly by polar and neutral residues (Fig. 4). One of the solvent

<sup>2</sup> M. M. Pereira and M. Teixeira, personal communication.

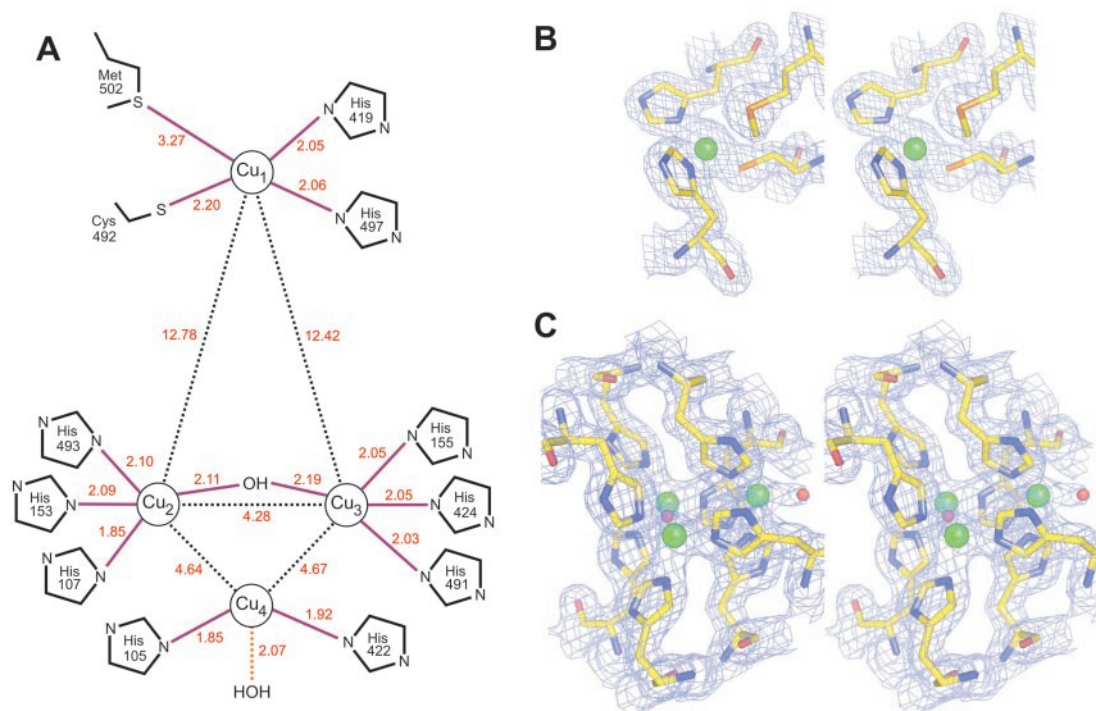


FIG. 3. **CotA copper centers.** A, schematic representation of the two copper centers, including interatomic distances among all the relevant atoms; B, stereo representation of the electronic density, resulting from the final refinement and contoured at 1.5σ, around the mononuclear copper center; C, stereo representation of the electronic density, resulting from the final refinement and contoured at 1.5σ, around the trinuclear copper center. In panels B and C, copper atoms and water molecules are represented as green and red balls, respectively.

TABLE III

Comparison of copper coordination distances among selected multicopper oxidases containing four copper atoms, and of known three-dimensional structure

MaLa structure was omitted because the presence of a dioxygen molecule as a bridge between Cu<sub>2</sub> and Cu<sub>3</sub> instead of an hydroxyl group.

Copper center	Protein				
	CotA	CueO	CcLa	TvLa	Asox
Mononuclear copper center Cu(1)					
Ligand 1	His <sup>419</sup> (2.05)	His <sup>443</sup> (2.02)	His <sup>457</sup> (1.87)	His <sup>395</sup> (2.36)	His <sup>512</sup> (2.05)
Ligand 2	Cys <sup>492</sup> (2.20)	Cys <sup>500</sup> (2.19)	Cys <sup>452</sup> (2.28)	Cys <sup>453</sup> (2.20)	Cys <sup>507</sup> (2.13)
Ligand 3	His <sup>497</sup> (2.06)	His <sup>505</sup> (1.98)	His <sup>396</sup> (1.91)	His <sup>458</sup> (2.23)	His <sup>445</sup> (2.09)
Ligand 4	Met <sup>502</sup> (3.27)	Met <sup>510</sup> (3.23)	Leu <sup>462</sup> (3.49)	Ile <sup>455</sup> (3.51)	Met <sup>217</sup> (2.90)
Trinuclear copper center					
Type 2 copper Cu(4)					
Ligand 1	His <sup>105</sup> (1.85)	His <sup>446</sup> (1.84)	Absent	His <sup>64</sup> (2.11)	His <sup>60</sup> (2.00)
Ligand 2	His <sup>422</sup> (1.92)	His <sup>101</sup> (1.92)	Absent	His <sup>398</sup> (1.97)	His <sup>448</sup> (2.09)
Ligand 3	HOH (2.07)	HOH (2.96)	Absent	HOH (2.58)	HOH (2.02)
Type 3 copper (binuclear)					
Cu(2)					
Ligand 1	His <sup>107</sup> (1.85)	His <sup>103</sup> (1.96)	His <sup>66</sup> (2.05)	His <sup>66</sup> (2.30)	His <sup>450</sup> (2.06)
Ligand 2	His <sup>153</sup> (2.09)	His <sup>141</sup> (1.97)	His <sup>109</sup> (1.98)	His <sup>109</sup> (2.53)	His <sup>106</sup> (2.16)
Ligand 3	His <sup>493</sup> (2.10)	His <sup>501</sup> (2.08)	His <sup>453</sup> (2.26)	His <sup>454</sup> (2.28)	His <sup>506</sup> (2.07)
Ligand 4	OH (2.19)	OH (2.43)	OH (2.13)	OH (1.98)	OH (1.99)
Cu(3)					
Ligand 1	His <sup>155</sup> (2.05)	His <sup>143</sup> (2.02)	His <sup>111</sup> (2.08)	His <sup>111</sup> (2.28)	His <sup>508</sup> (2.14)
Ligand 2	His <sup>424</sup> (2.05)	His <sup>448</sup> (1.94)	His <sup>401</sup> (2.06)	His <sup>400</sup> (2.11)	His <sup>62</sup> (1.98)
Ligand 3	His <sup>491</sup> (2.03)	His <sup>499</sup> (2.03)	His <sup>451</sup> (2.14)	His <sup>452</sup> (2.24)	His <sup>104</sup> (2.19)
Ligand 4	OH (2.11)	OH (2.29)	OH (3.12)	OH (1.97)	OH (2.06)
Cu(2)-Cu(3)	4.28	4.70	4.28	3.81	3.68
Cu(4)-Cu(2)	4.64	3.98		3.78	3.66
Cu(4)-Cu(3)	4.67	3.54		3.97	3.79
Cu(2)-O-Cu(3) Angle	168.5°	169.3°	139.9°	164.7°	130.9°

channels allows the communication between type II copper center and the protein surface, whereas the other one makes the connection between one of the copper atoms belonging to the type III copper center and the surface (Fig. 4). Messerschmidt *et al.* (18) described a similar configuration of solvent tunnels in the ascorbate oxidase structure. With the exception of MaLa laccase, in which a C-terminal plug occludes the exit of the solvent channel connecting type III copper center with the

protein surface (29), in all other analyzed multicopper oxidases the communication of the trinuclear copper center with the surface is mainly made by these two solvent tunnels. In CotA, the narrower channel connecting type II copper center with the protein surface, is slightly longer than in the other multicopper oxidases, with an overall length of ~13 Å.

*CotA Substrate Binding Site: Insights into Substrate Specificity*—The active centers of multicopper oxidases are cavities

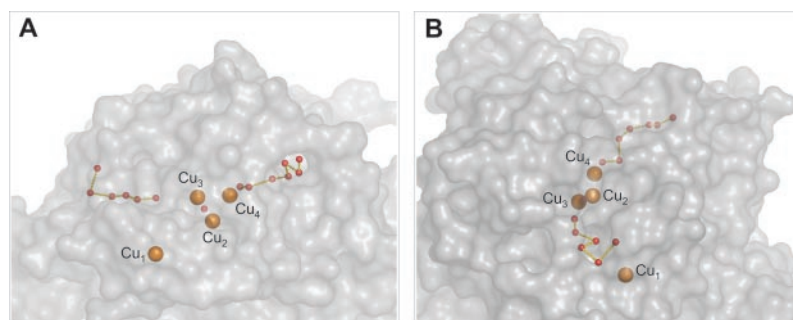


FIG. 4. Structure of CotA water channels which make possible the connection between the trinuclear copper center and the protein surface. Two water channels are characterized within the structure of CotA, establishing communication between the  $\text{Cu}_4$  (panel A) and  $\text{Cu}_3$  atoms (panel B) and the protein surface. These solvent channels are mainly surrounded by hydrophilic residues, which adopt a tunnel-like arrangement. Copper atoms and water molecules are represented as orange and red balls, respectively. The represented water molecules are related by hydrogen bonds.

close to the exposed mononuclear type I copper, responsible for the mono-electronic oxidations of a reducing substrate. A cavity analysis was performed with CASTP server (43), for CotA and for all other monomeric multicopper oxidases with known three-dimensional structures. Table IV lists the results of this analysis for six proteins in terms of the molecular and solvent-accessible areas and molecular and solvent-accessible volumes whereas Fig. 1 (panels D–F) depict a surface representation for CotA, CcLa, and CueO. The putative CotA substrate-binding site cavity has the largest values among the analyzed structures for all the calculated parameters. This is not surprising, because in CotA the cavity is not occluded by secondary structure elements (note that the lid-like structure mentioned above does not mask the substrate-binding site in the structure; Fig. 1, A and D). The opposite situation occurs in CueO, where this cavity has the lower values for any of the parameters listed in Table IV, as clearly visualized in Fig. 1C. Access to the copper I center in CueO is blocked to high molecular weight compounds because of the presence of a short  $\alpha$ -helix segment belonging to domain 2 (21). This helix defines a methionine-rich region proposed to provide binding sites for exogenous copper ions and with a role in the formation of a substrate-specific binding site (21). The putative substrate-binding cavity in CotA is mainly formed by apolar amino acids as in the CcLa laccase. This is in sharp contrast with the situation in the Asox and CueO proteins, in which substrate specificity imposes the presence of charged and polar residues in the active center of the enzymes (21). One possibility is that CotA functions to promote the cross-linking of small hydrophobic endospore coat protein components (see also “Discussion”).

**Thermostability Versus Structure**—Factors enhancing protein thermostability have been extensively reviewed elsewhere by the study of test case thermophilic proteins in comparison with their mesophilic counterparts (56). Several factors including hydrogen bonds and salt bridges, distribution of charged residues on the surface, protein packing, and amino acid composition have been postulated to be involved in the increased thermostability properties of some enzymes belonging to thermophilic microorganisms (57). In the particular case of CotA, all these factors were carefully analyzed in comparison with other monomeric multicopper oxidases of known three-dimensional structure. One feature that we analyzed was the proline content, which appears to be associated with increased protein thermostability (56). CotA contains 46 proline residues (8.9% of the total number of residues sequence), a number that does not differ greatly from that observed for other laccases of known structure (8% for TvLa, 7.5% for CcLa, and 8.2% for MaLa), all of which are considerably less thermostable than CotA (see Ref. 16 and references therein). However, the protein with the closest fold to CotA is not one of the structurally characterized

TABLE IV  
Analysis of surfaces and volumes of the putative substrate binding pockets of monomeric multicopper oxidases containing four copper atoms, as calculated by the CASTP server (43)

	Solvent-accessible area	Molecular surface area	Solvent-accessible volume	Molecular volume
	$\text{Å}^2$	$\text{Å}^2$	$\text{Å}^3$	$\text{Å}^3$
CotA	468	743	508	1346
CueO	28	138	6	116
CcLa	206	383	143	546
TvLa	112	285	49	268
MaLa	74	336	14	268
Asox	60	255	12	214

laccases, but the copper tolerance protein CueO (21, 58). Even taking into account the differences in experimental details, CueO does not appear to be as thermostable as CotA (59). CueO has a significantly lower proline content (6.2%) when compared with CotA. Thus, for a very similar fold, the higher proline content of CotA may be a factor promoting increasing thermostability (see also below).

On what concerns surface charge distribution, the majority of the analyzed structures showed a preferential presence of negatively charged residues on the surface, with no significant differences among them. However, CotA has a positive patch in the surface region located at the interface between domains 1 and 2. The significance of this positively charged patch is presently unknown, but we speculate that it may be involved in the recruitment of CotA to the coat structure (see “Discussion”). In some well documented cases, domain packing has been described as a major factor related with protein thermostability (60). A domain analysis carried out using the DOMID server, based on the quantification of local atomic interactions (45), was performed for CotA and for all the multicopper oxidases of known structure. In the eukaryotic proteins (Asox, CcLa, and TvLa), the overall fold determines the presence of three structurally independent cupredoxin-like domains (see above). However, in the bacterial multicopper oxidases (CueO and CotA), the overall arrangement of the cupredoxin-like domains suggested by this analysis corresponds to a highly packed structure in which only domain 3, containing the type I mononuclear copper center, can be clearly defined as an independent domain. A larger number of hydrophobic interactions between putative domains 1 and 2 are responsible, in the bacterial proteins, for the higher degree of domain packing in these enzymes. Moreover, and as pointed above, external connections contribute to the overall packing of both the CotA (this work) and CueO structures (21) (Fig. 1, A and C).

To allow a better understanding of these features, the atomic packing in CotA was analyzed. Atomic packing has been rec-

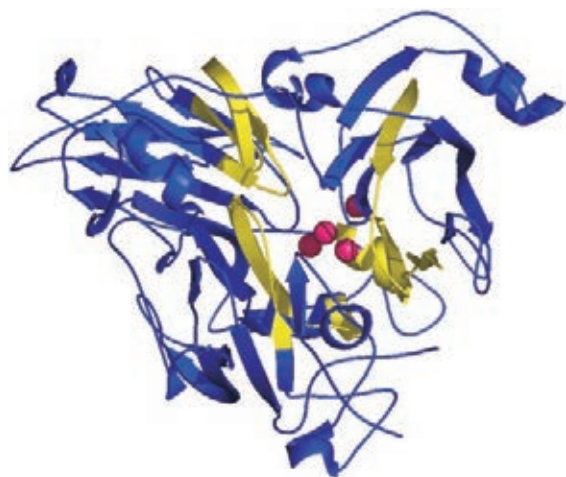


FIG. 5. Ribbon representation of the CotA structure, with the localization of the residues with higher OSP values (represented in yellow). Residues showing higher OSP values are arranged around the two copper centers, indicating that the protein core is tightly packed. Copper atoms are represented as magenta balls.

ognized as an important measurement for characterizing protein structure, because the observation that the interior of proteins is tightly packed with density similar to those observed in the crystals of small organic molecules (61). Studies of density within protein cores have implicated the so-called “packing efficiency” as an important factor determining protein thermostability (62). Several methods for determining atomic packing have been described in the literature, but one of the most widely employed is based on the calculation of the occluded surface for each protein residue, a powerful method that provides information on all atoms defining the packing environment of a particular atom (63). Following this method, the OSP for each CotA residue was calculated using the OS program (46). This parameter can be interpreted as a quantification of the accessibility to the solvent of each particular protein residue. This calculation was also performed, for comparison, for CueO and CcLa, and plotted together against the residue number (Fig. 5). OSP values for CotA protein showed three intervals in which this value corresponded to a more packed structure than in the other analyzed multicopper oxidases. These intervals correspond to residues 140–165, 275–300, and to the C-terminal segment containing residues 470–510 of CotA (see Fig. 2). These highly packed residues are localized in the interface regions between domains 1 and 2, and close to the mononuclear copper center (Fig. 5). All together, they constitute a pocket around the copper atoms, and contribute for the overall structure packing of CotA protein.

#### DISCUSSION

Multicopper proteins are ubiquitous enzymes, which catalyze oxidation reactions in organisms ranging from bacteria to humans (52). Despite their wide taxonomic distribution and diversity of substrates utilized, multicopper oxidases share a common fold, mainly constituted by three blocks (see above), which has probably evolved from a common monodomain ancestor (49). CotA from *B. subtilis* belongs to the multicopper oxidase family and recently has been characterized as a thermostable laccase (3, 16). The CotA structure solution by x-ray crystallography has provided a method to determine the possible role of this enzyme within the endospore coat.

CotA folding determined from the crystallographic data is very similar to the observed in other multicopper oxidases (27, 29, 58). An unique feature of CotA structure among the analyzed multicopper oxidases is the presence of a lid-like seg-

ment, composed by a loop and a short helix fragment, over the mononuclear copper center (Fig. 1A). We note, however, that a much shorter protruding coiled region of 6 residues was recently described in the TvLa structure (28, 54). This external loop is located surrounding the substrate binding site cavity close to type I copper center, and has been postulated to be involved in the closure of the substrate binding site induced by the protein-substrate interaction (28). Similarly, the lid-like segment in CotA, over the substrate binding cavity, may be also involved in the substrate binding process. An alternative explanation is that this region of the protein is involved in the assembly of CotA into the spore coat. However, we favor the first interpretation, as an analysis of the B values for this region is consistent with a flexible region involved in substrate binding.

Detailed structural comparison of CotA model with other monomeric multicopper oxidases has pointed out a larger number of hydrophobic interactions between the three constituting cupredoxin-like domains, which could be involved in the increased thermostability of the enzyme. Moreover, this characteristic was also observed in CueO protein, in which only domain 3, containing the type I copper center, can be defined as an independent domain (58). We suggest that the increased packing of CotA mediated by the interface regions between domains 1 and 2 and by the C-terminal end, is an important determinant in the remarkable thermostability of CotA. Interestingly, these segments contain only 4 of the 46 prolines present in CotA. Thus, if the proline content is a factor of the thermostability for CotA, then it may act in concert with the increased packing of CotA to promote its thermostability (56, 57). In despite of this consideration, individual atomic occluded surface packing values showed unambiguously the presence of a high packed atomic core around copper centers, which could be also related with the increased thermostability properties of the enzyme (62). Other as yet unidentified factors may also contribute to the remarkable thermostability of CotA.

Little is known about the *in vivo* substrate(s) of CotA. Expression of the *cotA* gene is required for the accumulation of a dark, melanin-like pigment by sporulating *B. subtilis* (15, 31). Laccases have been implicated in melanin biosynthesis in several fungi (64–67), and CotA has been shown to have laccase activity (3, 16). CotA may act as a classical laccase in the context of the multiprotein coat structure. However, yet another possibility is that CotA promotes the cross-linking of other coat structural components. Laccases have been implicated in the cross-linking of tyrosine-containing proteins (68). Moreover, *o,o*-dityrosine cross-links have been detected in purified coat material (1, 2), and that oxidative cross-linking has already been proposed for the tyrosine-rich CotG and CotC proteins (2, 69), both of which are, like CotA, outer spore components (8, 70). Another coat protein, CotU (71), is highly similar to CotC. Both are tyrosine-rich (30.3 and 27.9%, respectively) relatively small proteins (66 residues or 8.8 kDa for CotC, and 86 residues or 11.6 kDa for CotU). It is tempting to speculate that these proteins undergo cross-linking, and to suggest the involvement of CotA. This notion is supported by the architecture of the CotA active site, which seems designed for the accommodation of apolar, relatively large compounds. However, it is not presently known whether CotC or CotU undergo multimerization, or whether their assembly is in any way dependent on CotA.

In terms of three-dimensional structure, CotA is more similar to CueO from *E. coli*; however, both of the proteins have unrelated functions. CueO is a protein secreted to the periplasm of the Gram-negative cell, where it plays a role in

copper homeostasis (21, 58) whereas CotA is produced in the mother cell compartment of the sporulating Gram-positive cell and is recruited for assembly into the coat soon after its synthesis. Nevertheless, the two prokaryotic proteins share a very similar overall fold (Fig. 1; see also above). We speculate that CueO and CotA may be founding members of a prokaryotic-type fold of multicopper oxidases, which in the case of CotA may have been subjected to particular evolutionary constraints, as the protein has to fit into the highly ordered and dense multiprotein coat structure. We note that, whereas the bacterial spore is notorious for its heat resistance (1, 2), *cotA* has no role in this spore property. A *cotA* null mutant shows normal heat resistance (15). It is thus possible that the assembly of CotA has imposed a specific surface pattern that has translated into more internal changes that have increased the packing of the protein. We speculate that the high thermostability exhibited by CotA is an indirect consequence of these constraints. If so, then it may be possible to find other coat-associated thermostable enzymes. That seems to be the case, as highly stable spore-associated catalase isozymes have been reported (72, 73).

In any case, the interactions involved in the recruitment of CotA to the coat are unknown. Assembly of CotA may involve a large number of contacts dispersed along its surface as implied above, a specific region of the protein, or a combination of the two mechanisms. The CotE morphogenetic protein is responsible for the assembly of the spore outer coat layer (8). The available evidence indicates that residues in the C-terminal region of the 181-amino acid-long CotE protein mediate interactions with at least some of the proteins that are assembled in a CotE-dependent manner (9). In particular, residues 155–158 of CotE have been shown to be important for the assembly of CotA, as well as of other coat proteins (9). This region of CotE is acidic and is embedded in a larger region containing a high proportion of negatively charged amino acids (<sup>151</sup>DWEED-DEEDWEDELDEE<sup>166</sup>; residues 155–158 are underlined). It is presently not known whether CotE directly interacts with CotA, but we speculate that CotE may recruit CotA via an interaction between the region centered in residues 155–158, and the positively charged surface patch in CotA (see above). These and other predictions can now be tested by appropriate genetic screenings and site-directed mutagenesis.

**Acknowledgments**—Access to the EMBL Hamburg Facility is supported through the European Commission program “Access to Research Infrastructure Action of the Improving Human Potential Program” (Contract HPRI-1999-CT-00017). We thank the European Synchrotron Radiation Facility (Grenoble, France) and the joint support Structural Biology Group for the provision of data collection facilities at beamline ID14-EH2. We thank Dr. E. Pohl for excellent technical assistance during data collection and structure solution, and Dr. P. Lindley, Dr. C. Soares, and Dr. P. M. Matias for helpful discussions.

## REFERENCES

- Driks, A. (1999) *Microbiol. Mol. Biol. Rev.* **63**, 1–20
- Henriques, A. O., and Moran, C. P. J. (2000) *Methods Companion Methods Enzymol.* **20**, 95–110
- Hullo, M.-F., Moszer, I., Danchin, A., and Martin-Verstraete, I. (2001) *J. Bacteriol.* **183**, 5426–5430
- Ichikawa, H., and Kroos, L. (2000) *J. Biol. Chem.* **275**, 13849–13855
- Kroos, L., and Yu, Y. T. (2000) *Curr. Opin. Microbiol.* **3**, 553–560
- Ozin, A., Costa, T. V., Henriques, A. O., and Moran, C. P. J. (2001) *J. Bacteriol.* **183**, 2032–2040
- Ozin, A. J., Henriques, A. O., Hi, H., and Moran, C. P. J. (2000) *J. Bacteriol.* **182**, 1828–1833
- Zheng, L., Donovan, W. P., Fitz-James, P. C., and Losick, R. (1988) *Genes Dev.* **2**, 1047–1054
- Little, S., and Driks, A. (2001) *Mol. Microbiol.* **42**, 1107–1120
- Isticato, R., Cangiano, G., Tran, H. T., Ciabattini, A., Medaglini, D., Oggioni, M. R., Felice, M. d., Pozzi, G., and Ricca, E. (2001) *J. Bacteriol.* **183**, 6294–6301
- Brossier, F., Levy, M., and Mock, M. (2002) *Infect. Immun.* **70**, 661–664
- Henriques, A. O., Beall, B. W., Roland, K., and Moran, C. P. J. (1995) *J. Bacteriol.* **177**, 3394–3406
- Seyler, R., Henriques, A. O., Ozin, A., and Moran, C. P. J. (1997) *Mol. Microbiol.* **25**, 955–966
- Ozin, A. J., Samford, C. S., Henriques, A. O., and Moran, C. P. J. (2001) *J. Bacteriol.* **183**, 3041–3049
- Donovan, W., Zheng, L. B., Sandman, K., and Losick, R. (1987) *J. Mol. Biol.* **196**, 1–10
- Martins, L. M., Soares, C. M., Pereira, M. M., Teixeira, M., Jones, G. H., and Henriques, A. O. (2002) *J. Biol. Chem.* **277**, 18849–18859
- Xu, F. (1996) *Biochemistry* **35**, 7608–7614
- Messerschmidt, A., Ladenstein, R., Huber, R., Bolognesi, M., Avigliano, L., Petruzzelli, R., Rossi, A., and Finazzi-Agro, A. (1992) *J. Mol. Biol.* **224**, 179–205
- Zaitsev, I., Zaitsev, V., Card, G., Moshkov, K., Bax, B., Ralph, A., and Lindley, P. (1996) *J. Biol. Inorg. Chem.* **1**, 15–23
- Francis, C. A., and Tebo, B. M. (2001) *Appl. Environ. Microbiol.* **67**, 4272–4278
- Roberts, S. A., Weichsel, A., Grass, G., Thakali, K., Hazzard, J. T., Tollin, G., Rensing, C., and Montfort, W. R. (2002) *Proc. Natl. Acad. Sci. U. S. A.* **99**, 2766–2771
- Blackburn, N. J., Ralle, M., Hasset, R., and Kosman, D. J. (2000) *Biochemistry* **39**, 2316–2324
- McGuire, M. A., and Dooley, D. M. (1999) *Curr. Opin. Chem. Biol.* **3**, 138–144
- Alexandre, G., and Bally, R. (1999) *FEMS Microbiol. Lett.* **174**, 371–378
- Sanchez-Amat, A., and Solano, F. (1997) *Biochem. Biophys. Res. Commun.* **240**, 787–792
- Alexandre, G., and Zhulin, I. B. (2000) *Trends Biotech.* **18**, 41–42
- Ducros, V., Brzozowski, A. M., Wilson, K. S., Brown, S. H., Østergaard, P., Schneider, P., Yaver, D. S., Pedersen, A. H., and Davies, G. J. (1998) *Nat. Struct. Biol.* **5**, 310–316
- Bertrand, T., Jolival, C., Briozzo, P., Caminade, E., Joly, N., Madzak, C., and Mougou, C. (2002) *Biochemistry* **41**, 7325–7333
- Hakulina, N., Kiiskinen, L.-L., Kruus, K., Saloheimo, M., Paananen, A., Koivula, A., and Rouvinen, J. (2002) *Nat. Struct. Biol.* **9**, 601–605
- Huang, H.-W., Zoppellaro, G., and Sakurai, T. (1999) *J. Biol. Chem.* **274**, 32718–32724
- Rogolsky, M. (1968) *J. Bacteriol.* **95**, 2426–2427
- Riesenman, P. J., and Nicholson, W. L. (2000) *Appl. Environ. Microbiol.* **66**, 620–626
- Enguita, F. J., Matias, P. M., Martins, L. O., Plácido, D., Henriques, A. O., and Carrondo, M. A. (2002) *Acta Crystallogr. Sect. D Biol. Crystallogr.* **58**, 1490–1493
- Terwilliger, T. C., and Berendzen, J. (1999) *Acta Crystallogr. Sect. D Biol. Crystallogr.* **55**, 849–861
- Terwilliger, T. C. (2001) *Acta Crystallogr. Sect. D Biol. Crystallogr.* **57**, 1755–1762
- Cowtan, K. (1994) *Joint CCP4 ESF-EACBM Newsl. Protein Crystallogr.* **31**, 34–38
- Perrakis, A., Morris, R., and Lamzin, V. S. (1999) *Nat. Struct. Biol.* **6**, 458–463
- McRee, D. E. (1999) *J. Struct. Biol.* **125**, 156–165
- Murshudov, G. N., Lebedev, A., Vagin, A. A., Wilson, K. S., and Dodson, E. J. (1999) *Acta Crystallogr. Sect. D Biol. Crystallogr.* **55**, 247–255
- Laskowsky, R. A., MacArthur, M. W., Moss, D. S., and Thornton, J. M. (1993) *J. Appl. Crystallogr.* **26**, 283–291
- Hooft, R. W. W., Vriend, G., Sander, C., and Abola, E. E. (1996) *Nature* **381**, 272–276
- Sanner, F., Olson, A. J., and Sehner, J.-H. (1996) *Biopolymers* **38**, 305–320
- Liang, J., Edelsbrunner, H., and Woodward, C. (1998) *Protein Sci.* **7**, 1884–1987
- DeLano, W. L. (2002) *PyMol*, DeLano Scientific, San Carlos, CA
- Lu, H. (1999) [bioinfo1.mbfys.lu.se/Domid/domid.html](http://bioinfo1.mbfys.lu.se/Domid/domid.html)
- Pattabiraman, N., Ward, K. B., and Fleming, P. J. (1995) *J. Mol. Recog.* **8**, 334–344
- Gouet, P., Courcelle, E., Stuart, D. I., and Metz, F. (1999) *Bioinformatics* **15**, 305–308
- Corpet, F. (1988) *Nucleic Acids Res.* **16**, 10881–10890
- Murphy, M. E. P., Lindley, P. F., and Adman, E. T. (1997) *Protein Sci.* **6**, 761–770
- Lindley, P. F. (2001) in *Handbook of Metalloproteins* (Bertini, I., Sigel, A., and Sigel, H., ed) pp. 763–811, Marcel Dekker, Inc., New York
- Sali, A., and Blundell, T. L. (1993) *J. Mol. Biol.* **234**, 779–815
- Gray, H. B., Malmstrom, B. G., and Williams, R. J. (2000) *J. Biol. Inorg. Chem.* **5**, 551–559
- Palmer, A. E., Lee, S. K., and Solomon, E. I. (2001) *J. Am. Chem. Soc.* **123**, 6591–6599
- Piontek, K., Antorini, M., and Choinowski, T. (2002) *J. Biol. Chem.* **277**, 37663–37669
- Messerschmidt, A., Luecke, H., and Huber, R. (1993) *J. Mol. Biol.* **230**, 997–1014
- Kumar, S., Tsai, C.-J., and Nussinov, R. (2000) *Protein Eng.* **13**, 179–191
- Kumar, S., and Nussinov, R. (2001) *Cell. Mol. Life Sci.* **58**, 1216–1233
- Grass, G., and Rensing, C. (2001) *Biochem. Biophys. Res. Commun.* **286**, 902–908
- Kim, C., Lorenz, W. W., Hoopes, J. T., and Dean, J. F. D. (2001) *J. Bacteriol.* **183**, 4866–4875
- DeDecker, B. S., O'Brien, R., Fleming, P. J., Geiger, J. H., Jackson, S. P., and Sigler, P. B. (1996) *J. Mol. Biol.* **264**, 1072–1084
- Richards, F. M. (1974) *J. Mol. Biol.* **82**, 1–14
- Richards, F. M., and Lim, W. A. (1994) *Q. Rev. Biophys.* **26**, 423–498
- Fleming, P. J., and Richards, F. M. (2000) *J. Mol. Biol.* **299**, 487–498
- Eggert, C., Temp, U., Dean, J. F. D., and Eriksson, K.-E. L. (1995) *FEBS Lett.* **376**, 202–206
- Edens, W. E., Goins, T. G., Doodley, D., and Henson, J. M. (1999) *Appl. Environ. Microbiol.* **65**, 3071–3074
- Williamson, P. R., Wakamatsu, K., and Ito, S. (1998) *J. Bacteriol.* **180**, 1570–1572

67. Tsai, H.-F., Wheeler, M. H., Chang, Y. C., and Kwon-Chung, K. J. (1999) *J. Bacteriol.* **181**, 6469–6477
68. De Marco, A., and Roubelakis-Angelakis, K. A. (1997) *Phytochemistry* **46**, 421–425
69. Henriques, A. O., Melsen, L. R., and Moran, C. P. J. (1998) *J. Bacteriol.* **180**, 2285–2291
70. Sacco, M., Ricca, E., Losick, R., and Cutting, S. M. (1995) *J. Bacteriol.* **177**, 372–377
71. Lai, E. M., Phadke, N. D., Kachman, M. T., Giorno, R., Vazquez, S., Vazquez, J. A., Maddock, J. R., and Driks, A. (2003) *J. Bacteriol.* **185**, 1443–1454
72. Lawrence, N. L., and Halvorson, H. O. (1954) *J. Bacteriol.* **68**, 334–337
73. Norris, J. R., and Baillie, A. (1964) *J. Bacteriol.* **88**, 264–265